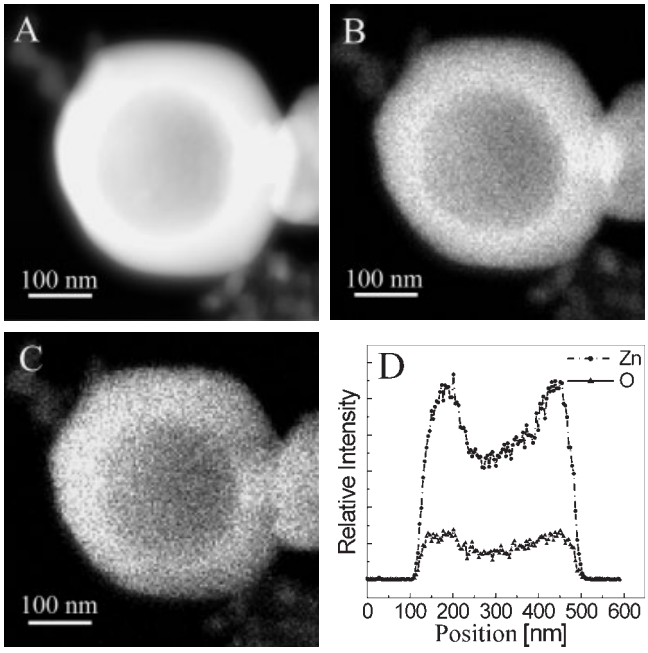

Figure 3. A) STEM image of one polyhedral ZnO hollow bead and elemental maps of Zn (B) and O (C) concentration. D) Cross-sectional compositional line profiles of the hollow bead shown in (A).

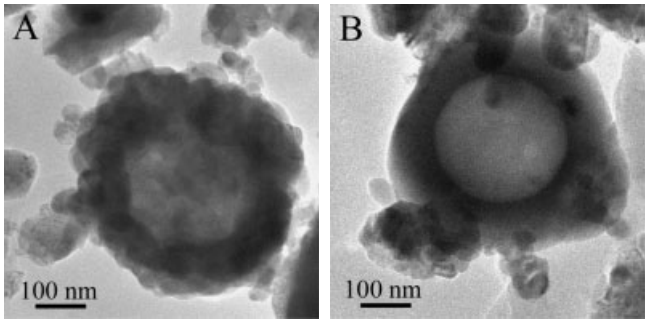

Figure 4. TEM images of some in-process shapes observed in the products collected in the different temperature zones: A) at about 400 °C; B) at about 500 °C.

inserted into a tube furnace preheated to 600–700 °C. The Zn powder was kept about 5 cm below the high-temperature zone of the tube furnace, as shown in the left portion of Figure 1. All the experiments were carried out under atmospheric pressure. The fundamental output of a Q-switched Nd:YAG laser (Quantary DCR 130), 1064 nm in wavelength and 7 ns in pulse width, was gently focused on Zn by a long-focal-length lens to generate the mixture of Zn clusters and ethanol droplets. After 5 min of laser ablation, the tube was cooled down to room temperature, and the gray deposits on the walls of the quartz tube were carefully collected.

X-ray diffraction measurements were performed on a Rigaku D-max/RC diffractometer using Cu Kα radiation. The morphology of the products was investigated using transmission electron microscopy (Tecnai F30). Energy-dispersive X-ray characterization and elemental mapping were performed with an EDX system attached to a Tecnai F30 TEM.

Received: December 16, 2003
Final version: March 3, 2004

[1] S. J. Oldenburg, G. D. Hale, J. B. Jackson, N. J. Halas, *Appl. Phys. Lett.* **1999**, *75*, 1063.
[2] S. W. Kim, M. Kim, W. Y. Lee, T. Hyeon, *J. Am. Chem. Soc.* **2002**, *124*, 7642.
[3] Y. G. Sun, B. Mayers, Y. N. Xia, *Adv. Mater.* **2003**, *15*, 7.
[4] Q. Peng, Y. J. Dong, Y. D. Li, *Angew. Chem. Int. Ed.* **2003**, *42*, 3027.
[5] E. Mathiowitz, J. S. Jacob, Y. S. Jong, G. P. Carino, D. E. Chickering, P. Chaturvedi, C. A. Santos, K. Vijayaraghavan, S. Montgomery, M. Bassett, C. Morrell, *Nature* **1997**, *386*, 410.
[6] F. Caruso, *Top. Curr. Chem.* **2003**, *227*, 145.
[7] E. Baumeister, S. Klaeger, *Adv. Eng. Mater.* **2003**, *5*, 673.
[8] M. Ueda, M. Seno, K. Tanizawa, S. Kuroda. *Nat. Biotechnol.* **2003**, *21*, 885.
[9] H. Ai, S. A. Jones, Y. M. Lvov, *Cell Biochem. Biophys.* **2003**, *39*, 23.
[10] Y. Hu, J. F. Chen, W. M. Chen, X .H. Lin, X. L. Li, *Adv. Mater.* **2003**, *15*, 726.
[11] F. Caruso, *Adv. Mater.* **2001**, *13*, 11.
[12] A. K. Boal, F. Ilhan, J. E. DeRouchey, T. Thurn-Albrecht, T. P. Russell, V. M. Rotello, *Nature* **2000**, *404*, 746.
[13] B. L. Frankamp, O. Uzun, F. Ilhan, A. K. Boal, V. M. Rotello, *J. Am. Chem. Soc.* **2002**, *124*, 892.
[14] J. X. Huang, Y. Xie, B. Li, Y. Liu, Y. T. Qian, S. Y. Zhang, *Adv. Mater.* **2000**, *12*, 808.
[15] R. A. Caruso, *Top. Curr. Chem.* **2003**, *226*, 91.
[16] Z. Z. Yang, Z. W. Niu, Y. F. Lu, Z. B. Hu, C. C. Han, *Angew. Chem. Int. Ed.* **2003**, *42*, 1943.
[17] J. N. Cha, H. Birkedal, L. E. Euliss, M. H. Bartl, M. S. Wong, T. J. Deming, G. D. Stucky, *J. Am. Chem. Soc.* **2003**, *125*, 8285.
[18] Y. G. Sun, B. T. Mayers, Y. N. Xia, *Nano Lett.* **2002**, *2*, 481.
[19] P. X. Gao, Z. L. Wang, *J. Am. Chem. Soc.* **2003**, *125*, 11 299.
[20] C. R. Wang, K. B. Tang, Q. Yang, J. Q. Hu, Y. T. Qian, *J. Mater. Chem.* **2002**, *12*, 2426.
[21] D. H. Chen, D. R. Chen, X. L. Jiao, Y. T. Zhao, *J. Mater. Chem.* **2003**, *13*, 2266.
[22] Z. Q. Li, Y. Xie, Y. J. Xiong, R. Zhang, *New J. Chem.* **2003**, *27*, 1518.
[23] M. H. Huang, S. Mao, H. N. Feick, H. Q. Yan, Y. Y. Wu, H. Kind, E. Weber, R. Russo, P. D. Yang, *Science* **2001**, *292*, 1897.

Self-Assembling Polymer–Peptide Conjugates: Nanostructural Tailoring**

By *Joel H. Collier* and *Phillip B. Messersmith**

Self-assembly of proteins, small peptides, and peptidomimetics into supramolecular β-sheet fibrils is an increasingly utilized route for the synthesis of new nanostructured materials.[1–6] These self-assembled fibrillar structures lend themselves to a wide range of applications, as illustrated by their

[*] Prof. P. B. Messersmith, J. H. Collier
Department of Biomedical Engineering, Northwestern University
2145 Sheridan Road, Room E310
Evanston, IL 60208, 847-467-5273 (USA)
E-mail: philm@northwestern.edu

[**] We thank Annelise Barron for use of the peptide synthesizer, Mark Johnson, Bert Menco and Jiahn-Dar Huang for assistance with QFDE, and Arthur Veis for use of the TEM. This research was supported by NIH grant DE 13030.

DOI: 10.1002/adma.200306379

ADVANCED MATERIALS

recent use as templates for producing nanoscale electronic components[5,7] and for constructing hydrogels for tissue engineering and other biomedical applications.[1,8,9] One shortcoming of this developing technology, however, is that in almost all cases, self-assembled β-sheet fibrils have a propensity for uncontrollably aggregating into disordered tangles. Although a few amyloids show less lateral aggregation than others,[5] this uncontrollable lateral aggregation is a general feature of self-assembling β-sheet peptides and proteins both in vivo and in vitro. Furthermore, β-sheet peptide fibrils are remarkably resistant to dimensional tailoring, as similar fibrils are produced by peptides of vastly differing sequences, lengths, and initial folding.[10] These properties dramatically limit the utility of these materials for applications where a more predictable or modifiable fibrillar configuration is necessary. To address this issue, we designed and investigated the solution behavior of a series of peptide–polymer conjugates that self-assemble via β-sheet fibril formation, identifying a poly(ethylene glycol) (PEG)-conjugated peptide that self-assembles into very uniform fibrils with little to no lateral aggregation. Quick-freeze deep-etch transmission electron microscopy (QDFE-TEM) showed that this peptide–polymer formed aligned and uniformly spaced fibrils with a much greater degree of three-dimensional regularity than is typically seen in β-sheet fibril-based self-assembled materials. This approach is potentially useful for tailoring β-sheet-forming peptide materials for a wide range of applications, including nanoelectronic components and biomedical materials.

Because β-sheet formation involves intermolecular hydrogen bonding between amide N–H and C=O groups, we hypothesized that inserting non-peptide random-coil-forming polymers within the peptide backbone could modulate β-sheet fibril dimensions such as width, length, or lateral aggregation. This hypothesis was also based in part on the previous work by Burkoth and co-workers, who showed that PEG-modified $A\beta_{(10-35)}$ formed thin, soluble fibrils that aggregated to a much lesser extent than unmodified $A\beta_{(10-35)}$ in solution and when dried onto TEM grids.[11,12] Here, we synthesized a series of PEG–peptides with various PEG blocks incorporated within the backbone structure of the molecule (Fig. 1). The longest peptide, Ac–QQKFQFQFEQQ–Am (Q11), has been shown to form β-sheet fibrils in aqueous solutions and was developed previously as a self-assembling transglutaminase substrate for enzymatic biofunctionalization of the supramolecular structure.[9] Further, it is also phenylalanine-rich, a property that has been indicated to be potentially important in β-sheet fibril formation.[13] Other molecules studied here include a 7-amino acid peptide representing the central core of Q11 (Ac–KFQFQFE–Am, Q7), two peptides with monodisperse oligo(ethylene glycol) (EG) chains integrated into the peptide backbone (EG_{12}–Q7 and Q7–EG_{12}–Q7), and a peptide with a polydisperse PEG chain attached at the c-terminus (Q11–PEG, PEG $M_w \approx 3700$ as shown by matrix-assisted laser desorption ionization time-of-flight mass spectrometry (MALDI-TOF-MS)). These five molecules were investigated to study the effect of both molecular architecture (triblock versus diblock) and the length of the PEG chain on the structures of their self-assemblies.

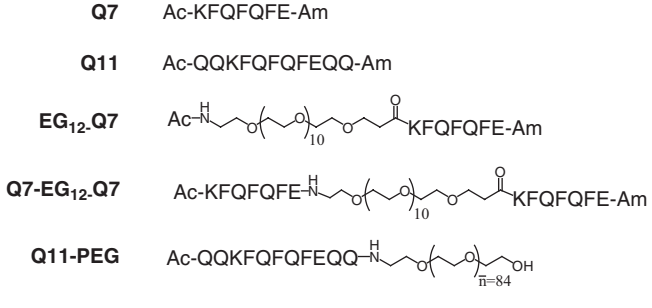

Figure 1. Self-assembling peptides and PEG–peptides.

When aqueous solutions of 4 % Q11, Q7, EG_{12}–Q7, or Q11–PEG were pipetted into salt-containing solutions such as phosphate-buffered saline (PBS, 0.2 g L^{-1} KCl, 0.2 g L^{-1} KH_2PO_4, 8 g L^{-1} NaCl, 1.15 g L^{-1} Na_2HPO_4, pH 7.4), these molecules self-assembled. This salt- and pH-sensitive self-assembly has been observed with similar peptides, where self-assembly occurs very rapidly in the presence of electrolytes or in certain pH ranges, but is retarded or absent in pure water.[14,15] Addition of Congo red to the salt solutions allowed direct visualization of the macroscopic structures. Q7 and Q11 formed three-dimensional hydrogels in PBS, similar to previously observed peptides.[9,14] However, when aqueous solutions of EG_{12}–Q7 were pipetted into PBS, the structures that were formed were not cohesive, like those of Q7 and Q11, and instead formed fragmented Congo-red-stainable structures. When aqueous solutions of Q11–PEG were pipetted into PBS, no macroscopic hydrogels were observed, but subsequent TEM and spectroscopic studies revealed that Q11–PEG in fact formed soluble fibrillar structures. These soluble fibrils did not aggregate into a macroscopically observable Congo-red-stained hydrogel, as the constituent fibrils remained free in solution. In contrast to other peptides and PEG–peptides, Q7–EG_{12}–Q7 was not water-soluble. Instead, lyophilized Q7–EG_{12}–Q7 formed a white precipitate when added to water, and concentrated solutions of Q7–EG_{12}–Q7 in trifluoroacetic acid (TFA) formed suspensions of transparent solid fragments on the order of 10 μm–1 mm when added to water. Because of Q7–EG_{12}–Q7's insolubility and our focus of pursuing fibril-forming molecules, no further experiments were performed on Q7–EG_{12}–Q7.

Fourier transform infrared spectroscopy (FTIR) of aqueous solutions indicated high β-sheet contents for Q11, Q7, EG_{12}–Q7, and Q11–PEG (Fig. 2). All showed predominant peaks in the 1614–1620 cm^{-1} range, indicating a predominance of aggregated β-sheet strand structure.[16] Q11, Q7, and Q11–PEG also exhibited peaks in the 1684–1692 cm^{-1} range, suggesting the presence of antiparallel β-sheets. A small amount of helical character also appeared to be present, as evidenced by minor peaks at 1653 cm^{-1} (Q11), 1636 cm^{-1} (Q11-PEG), 1637 cm^{-1} (Q7), and 1635 cm^{-1} (EG_{12}–Q7). Trace amounts of TFA accounted for peaks seen at 1672 cm^{-1} in the spectra of

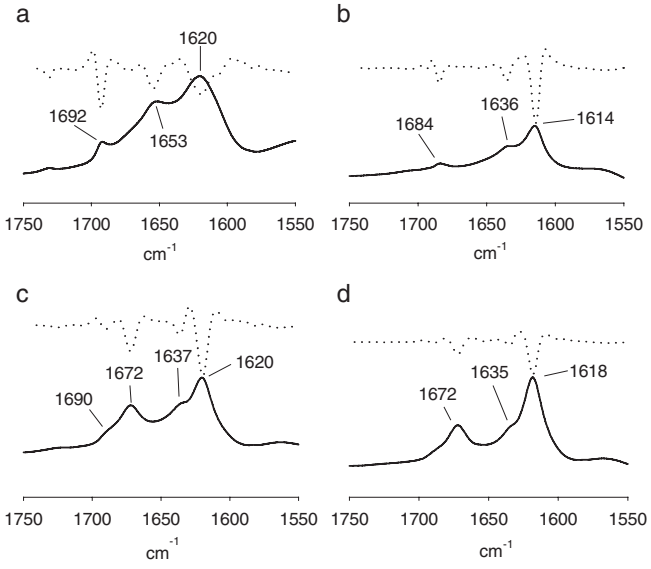

Figure 2. FTIR spectra (solid) and second-derivatives (dotted) of Q11 (a), Q11–PEG (b), Q7 (c), and EG_{12}–Q7 (d), 40 mg mL^{-1} in D_2O except Q11, which was 40 mg mL^{-1} in 1:1 D_2O:H_2O due to poor solubility of Q11 in D_2O.

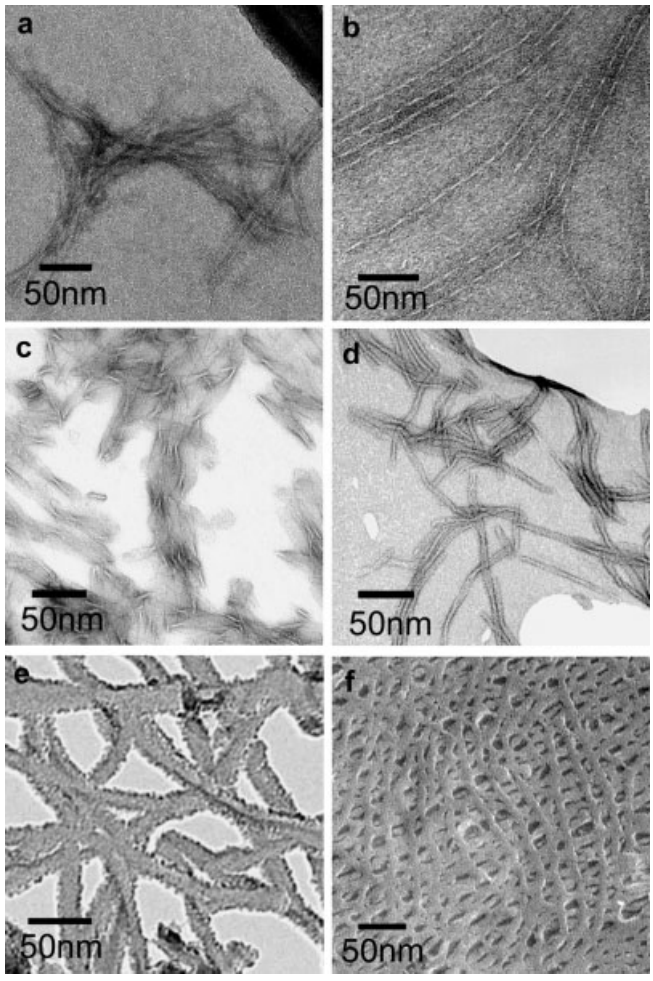

Figure 3. TEM images with negative staining of Q11 fibrils (a), Q11–PEG fibrils (b), Q7 twisted ribbons (c), and EG12–Q7 ribbons (d); QFDE images of Q11 fibrils (e), and Q11–PEG fibrils (f).

Q7 and EG_{12}–Q7. In short, the FTIR results point to considerable β-sheet content with a smaller helical component. This observation was also supported by circular dichroism (CD) spectroscopy, which showed a predominance of β-sheet character for Q7, Q11, EG_{12}–Q7, and Q11–PEG dissolved in water at a concentration of 100 μM (data not shown).

TEM of negatively stained self-assemblies revealed dramatically different fibrillar morphologies, especially between unmodified Q11 and Q11–PEG. Negatively stained TEM samples showed that Q11 formed fibrils with classical amyloid morphology: fibrils of ~10 nm in width, laterally aggregated into bundles and tangles (Fig. 3a). In stark contrast, Q11–PEG formed thinner, longer, and straighter fibrils that appeared to possess a regular helical twist with a pitch of about 20 nm (Fig. 3b). Also, these fibrils showed little to no lateral aggregation when dried onto TEM grids, instead running parallel to each other for hundreds of nanometers, often maintaining an even spacing of about 10–15 nm. This minimization of lateral aggregation has also been observed for PEGylated $A\beta_{(10-35)}$.[11,12] Q7 and EG_{12}–Q7 produced fibrils with morphologies similar to Q11 fibrils, with widths of about 10 nm and considerable lateral aggregation. Unlike Q11, however, Q7 (Fig. 3c) and EG_{12}–Q7 (Fig. 3d) tended to appear more tape-like, with Q7 especially showing a twisted-ribbon-like morphology. These twisted ribbons are similar to the nanostructures reported by Marini et al. with the short peptide FKFEFKFE.[17]

We also utilized QFDE-TEM, a technique that is more appropriate than negatively stained TEM for visualizing the three-dimensional arrangement of the fibrils in solution.[18] QFDE-TEM of Q11 revealed networks of highly entangled fibrils (Fig. 3e). These fibrils appeared somewhat disordered, with widths of 15–30 nm. In stark contrast to Q11, Q11–PEG formed much longer, straighter, more uniform, and less laterally aggregated fibrils (Fig. 3f). Like the Q11–PEG fibrils observed with negatively stained TEM, the fibrils seen with QFDE-TEM also ran parallel to each other for several hundreds of nanometers and maintained a characteristic spacing of about 10 nm between fibrils. This verified that the minimal lateral aggregation observed with negative-stained Q11–PEG samples was not simply an artifact of the drying process. Also, QFDE-TEM supported the observation that Q11–PEG fibrils were thinner than those of Q11. Whereas QFDE-TEM showed Q11 fibrils to be 15–30 nm in diameter, Q11–PEG were uniformly about 8 nm in diameter. Interestingly, deep-etching also enabled us to see the fibrils that lay beneath the top layer of fibrils. In many cases, these underlying fibrils ran at right angles to the top layer, suggesting that in solution these fibrils may pack into alternating layered fibril structures (Fig. 3f). The process by which the PEG chains exert their

ADVANCED MATERIALS

effect on the nanostructures of the formed fibrils is not clear, but possible mechanisms include the steric shielding of the fibrils by a PEG shell or the polydispersity of the PEG chains impeding PEG crystallization. Wider ranges of solution conditions than the ones explored here may yield more insight into the aligned fibril configuration seen with Q11–PEG. For example, experiments that vary the valency and/or ionic strength of the buffer electrolytes might lead to other configurations of Q11–PEG fibrils. QFDE-TEM of EG_{12}–Q7 and Q7, like the negatively stained samples, supported a tape-like structure with significant lateral aggregation (not shown).

In summary, we have shown that incorporation of PEG into the backbone of self-assembling β-sheet peptides is an effective means for modulating the nanoscale assembly of the fibrils, particularly their lateral aggregation, width, solubility, and uniformity. In particular, Q11–PEG produced the most dramatically different nanostructures from unmodified Q11. The ordered matrices produced by Q11–PEG are a significant departure from the typical structure of amyloid fibrils, which tend to form aggregates without the regular fibril spacing and alignment seen with Q11–PEG. Although some amyloids have been reported that laterally aggregate to lesser extents than other amyloids,[5] the PEGylation of β-sheet fibril-forming peptides may prove to be a more general approach for reducing lateral aggregation. The ability of PEG-modified β-sheet-forming peptides to form β-sheet structures has also been shown in previous studies,[12,19–21] and alternate chemistries for producing β-sheet peptide–PEG copolymers have been reported,[20,21] broadening the synthetic possibilities for producing these or similar molecules.

Experimental

All peptides and PEG–peptides were synthesized with solid-phase Fmoc techniques. For introducing monodisperse oligo(ethylene glycol) chains into the backbones of EG_{12}–Q7 and Q7–EG_{12}–Q7, we utilized the commercially available Fmoc-protected PEG amino acid *O*-(*n*-Fmoc-2-aminoethyl)-*O′*-(2-carboxyethyl)-undecaethylene glycol (NovaBiochem, cat#01–63–0109). For synthesizing Q11–PEG we utilized PAP Tentagel resin (Peptides International, cat# RTS-9002-PI). After peptide synthesis, acid cleavage from this resin yields a peptide with the PEG chain attached via an amide linkage [11,12]. Peptides and PEG–peptides were analyzed with reverse-phase high-performance liquid chromatography (HPLC) and MALDI-TOF mass spectrometry. Q11–PEG was additionally analyzed with amino acid analysis. All peptides and PEG–peptides were found to be ≥95 % pure.

FTIR spectroscopy was performed for concentrated peptides and PEG–peptides (40 mg mL^{-1} in D_2O) with a Biorad FTS-60 using a liquid cell with BaF_2 windows and 10 μm spacers. Q11 was water-soluble, but sparingly soluble in D_2O, so for this peptide 1:1 D_2O/H_2O was used. Sixteen scans were summed. For second-derivative calculations, the Savitsky–Golay method was used.

For TEM with negative staining, 30 mM aqueous solutions of peptides and PEG–peptides were mixed 1:2 in Dulbecco's phosphate buffered saline (PBS, Mediatech cat# 21–031, with 0.2 g L^{-1} KCl, 0.2 g L^{-1} KH_2PO_4, 8 g L^{-1} NaCl, 1.15 g L^{-1} Na_2HPO_4, pH 7.4, final peptide concentration 10 mM), vortexed, incubated on the bench top for 48 h, applied to lacey carbon grids, and stained with 1 % uranyl acetate.

For QFDE-TEM of Q7 and Q11, which form self-supporting gels, we incubated 30 mM aqueous peptide in a flip-top centrifuge tube under a layer of PBS for 3 days to allow the PBS to diffuse through the peptide solution and cause self-assembly. After 3 days, the PBS was removed from the gelled peptide layer, which was analyzed with QFDE-TEM. For QFDE of EG_{12}–Q7 and Q11–PEG, whose gels are more fragile (and as a result do not lend themselves to the layered-self-assembly approach described above), we dissolved the PEG–peptides in water at a concentration of 60 mM, mixed these solutions 1:1 with PBS, and incubated them for 3 days. In this way, the concentrations of all four peptides and PEG–peptides were consistent between QFDE samples, as were the concentrations of buffer constituents.

Received: October 29, 2003
Final version: March 10, 2004

[1] J. Kisiday, M. Jin, B. Kurz, H. Hung, C. Semino, S. Zhang, A. J. Grodzinsky, *Proc. Natl. Acad. Sci. USA* **2002**, *99*, 9996.
[2] C. E. MacPhee, C. M. Dobson, *J. Am. Chem. Soc.* **2000**, *122*, 12 707.
[3] H. A. Lashuel, S. R. LaBrenz, L. Woo, L. C. Serpell, J. W. Kelly, *J. Am. Chem. Soc.* **2000**, *122*, 5262.
[4] A. Aggeli, M. Bell, N. Boden, J. N. Keen, P. F. Knowles, T. C. McLeish, M. Pitkeathly, S. E. Radford, *Nature* **1997**, *386*, 259.
[5] T. Scheibel, R. Parthasarathy, G. Sawicki, X. M. Lin, H. Jaeger, S. L. Lindquist, *Proc. Natl. Acad. Sci. USA* **2003**, *100*, 4527.
[6] J. P. Schneider, D. J. Pochan, B. Ozbas, K. Rajagopal, L. Pakstis, J. Kretsinger, *J. Am. Chem. Soc.* **2002**, *124*, 15 030.
[7] M. Reches, E. Gazit, *Science* **2003**, *300*, 625.
[8] T. C. Holmes, S. de Lacalle, X. Su, G. Liu, A. Rich, S. Zhang, *Proc. Natl. Acad. Sci. USA* **2000**, *97*, 6728.
[9] J. H. Collier, P. B. Messersmith, *Bioconjugate Chem.* **2003**, *14*, 748.
[10] A. K. Chamberlain, C. E. MacPhee, J. Zurdo, L. A. Morozova-Roche, H. A. O. Hill, C. M. Dobson, J. J. Davis, *Biophys. J.* **2000**, *79*, 3282.
[11] T. S. Burkoth, T. L. S. Benzinger, D. N. M. Jones, K. Hallenga, S. C. Meredith, D. G. Lynn, *J. Am. Chem. Soc.* **1998**, *120*, 7655.
[12] T. S. Burkoth, T. L. S. Benzinger, V. Urban, D. G. Lynn, S. C. Meredith, P. Thiyagarajan, *J. Am. Chem. Soc.* **1999**, *121*, 7429.
[13] R. Azriel, E. Gazit, *J. Biol. Chem.* **2001**, *276*, 34 156.
[14] J. H. Collier, B. H. Hu, J. W. Ruberti, J. Zhang, P. Shum, D. H. Thompson, P. B. Messersmith, *J. Am. Chem. Soc.* **2001**, *123*, 9463.
[15] S. Zhang, T. Holmes, C. Lockshin, A. Rich, *Proc. Natl. Acad. Sci. USA* **1993**, *90*, 3334.
[16] P. I. Haris, in *Infrared Analyses of Peptides and Proteins: Principles and Applications*, ACS, Washington, DC **2000**, p. 190.
[17] D. M. Marini, W. Hwang, D. A. Lauffenburger, S. G. Zhang, R. D. Kamm, *Nano Lett.* **2002**, *2*, 295.
[18] J. Heuser, *Trends Biochem. Sci.* **1981**, *6*, 64.
[19] A. Rosler, H. A. Klok, I. W. Hamley, V. Castelletto, O. O. Mykhaylyk, *Biomacromolecules* **2003**, *4*, 859.
[20] Y. Fukushima, *J. Polym. Sci., Part A: Polym. Chem.* **2001**, *39*, 742.
[21] O. Rathore, D. Y. Sogah, *J. Am. Chem. Soc.* **2001**, *123*, 5231.

